Every Vote Counts: Ranking-Based Training of Federated Learning to Resist Poisoning Attacks

Hamid Mozaffari, Virat Shejwalkar, and Amir Houmansadr,
University of Massachusetts Amherst

This paper is included in the Proceedings of the 32nd USENIX Security Symposium.

August 9–11, 2023 • Anaheim, CA, USA

Every Vote Counts:
Ranking-Based Training of Federated Learning to Resist Poisoning Attacks

Hamid Mozaffari, Virat Shejwalkar, and Amir Houmansadr

University of Massachusetts Amherst

{hamid, vshejwalkar, amir}@cs.umass.edu

Abstract

Federated learning (FL) allows untrusted clients to collaboratively train a common machine learning model, called *global model*, without sharing their private/proprietary training data. However, FL is susceptible to *poisoning* by malicious clients who aim to hamper the accuracy of the global model by contributing malicious updates during FL's training process.

We argue that the key factor to the success of poisoning attacks against existing FL systems is the large space of model updates available to the clients to choose from. To address this, we propose *Federated Rank Learning* (FRL). FRL reduces the space of client updates from model parameter updates (a continuous space of float numbers) in standard FL to the space of parameter rankings (a discrete space of integer values). To be able to train the global model using parameter ranks (instead of parameter weights), FRL leverage ideas from recent *supermasks training* mechanisms. Specifically, FRL clients rank the parameters of a randomly initialized neural network (provided by the server) based on their local training data, and the FRL server uses a voting mechanism to aggregate the parameter rankings submitted by the clients.

Intuitively, our voting-based aggregation mechanism prevents poisoning clients from making significant adversarial modifications to the global model, as each client will have a single vote! We demonstrate the robustness of FRL to poisoning through analytical proofs and experimentation, and we show its high communication efficiency.[1]

1 Introduction

Federated Learning (FL) allows mutually untrusted *clients* (e.g., Android devices) to collaborate and train a common model, called *global model*, without sharing their private data. In a single FL round, a *server* (e.g., a Google server) broadcasts the current global model to a random subset of clients, the clients compute model updates using the global model and their private data, and share them with the server, server

---

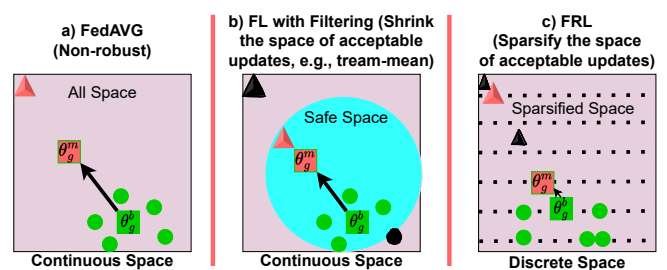[1]An extended version available at https://arxiv.org/abs/2110.04350

Figure 1: The space of client updates. Green circles represent benign updates and red triangles represent malicious updates. To defend against poisoning, existing robust AGRs filter the updates by creating a safe space (continuous $\in \mathbb{R}^d$). On the other hand, FRL limits the choices of clients by enforcing a discrete space of updates (a permutation of integers $\in [1, d]$). θ_g^b (green square) demonstrates the aggregated model for benign users, and θ_g^m (red square) demonstrates the aggregated model considering malicious updates. Black objects are updates that are ruled out by the server.

aggregates the updates using an *aggregation rule* (AGR) and updates the global model using the aggregate.

Robustness to poisoning attacks: Most of the distributed learning algorithms, including FedAvg [31] and FedProx [29], operate on mutually untrusted clients and server. This makes distributed learning susceptible to the threat of *poisoning* [10, 24, 39]. A *poisoning adversary* can either own or control a few of FL clients, called *malicious clients*, and instruct them to share malicious updates with the central server in order to reduce the performance of the global model. There are three approaches to poisoning FL: *targeted* [8, 41] attacks aim to reduce the utility of the global FL model on specific test inputs of adversary's choice; *untargeted* [5, 18, 38] attacks aim to reduce the utility of global model on arbitrary test inputs; and *backdoor* [4, 42, 44] attacks aim to reduce the utility on test inputs that contain a specific signal called the trigger. In our work, we focus on the more severe threat of untargeted poisoning [39], which, unlike targeted and backdoor poisoning, affects the majority FL clients.

High-level intuition of FL untargeted poisoning: Figure 1 shows how the poisoning adversary searches for malicious updates in the space of possible updates to maximize the distance between benign and malicious aggregates. When the server's AGR is not robust, e.g., dimension-wise average [31], there is no limitation on the adversary's choices, so they can maximize their goal using a malicious update arbitrarily far from benign updates; (Figure 1-a)). Therefore, even a single malicious client can jeopardize the accuracy of the global model trained using FedAvg [9]. Current robust AGRs, such as Multi-krum [9] or Trimmed-mean [45] limit the space of acceptable updates, i.e., the safe zone shown in Figure 1-b). These robust AGRs only consider the updates that are in the safe zone and thereby reduce the adversary's choices.

Continuous versus discrete space of updates: Figure 1-c) shows how our proposed defense (FRL, which is introduced next) limits the poisoning adversary's choices of malicious updates by making the space of acceptable updates *discrete*. To the best of our knowledge, most of previous Byzantine robust FL algorithms use a *continuous* space of updates ($\in \mathbb{R}^d$), as their frameworks are built on exchanging trained (32-bit) weight parameters. On the other hand, in our approach, the clients send their updates in the form of *edge rankings*, i.e., a permutation of integers $\in [1, d]$ where d is the size of the network layer; more useful edges have higher ranks. In Figure 1-c), the black dots show the discrete space of acceptable client updates. For example, a network with 4 edges can have 4! possible permutations of edge rankings starting from [1,2,3,4] to [4,3,2,1]. On the other hand, in FL algorithms with a continuous space of updates (with or without a safe zone), the adversary's choices are 4 weight parameters (each of 32 bits). Note that, sparsification of the space of acceptable updates is different from sparsification of model updates used in compression methods, e.g., TopK [3]), RandomK [40] and Sketched-SGD [23]. In these methods, the FL client sends only a fraction of model updates instead of all of them, but each parameter still has a continuous space.

Federated Rank Learning (FRL): We present FRL, a novel FL algorithm that concurrently achieves the two goals of robustness against poisoning attacks and communication efficiency. FRL uses a novel learning paradigm called *supermasks* training [35, 46] to create edge rankings, which, as we will show, allows FRL to reduce communication costs while achieving significantly stronger robustness. Specifically, in FRL, clients collaborate to find a *subnetwork* within a *randomly initialized* neural network which we call the *supernetwork* (this is in contrast to conventional FL where clients collaborate to *train* a neural network). The goal of training in FRL is to collaboratively rank the supernetwork's edges based on the importance of each edge and find a *global ranking*. The global ranking can be converted to a supermask, which is a binary mask of 1's and 0's, that is superimposed on the random neural network (the supernetwork) to obtain the final subnetwork. For example, in our experiments, the final

subnetwork is constructed using the top 50% of all edges. The subnetwork is then used for downstream tasks, e.g., image classification, hence it is equivalent to the global model in conventional FL. Note that in entire FRL training, weights of the supernetwork *do not* change.

More specifically, each FRL client computes the importance of the edges of the supernetwork based on their local data. The importance of the edges is represented as a ranking vector. Each FRL client will use the *edge popup* algorithm [35] and their data to compute their local rankings (the edge popup algorithm aims at learning which edges in a supernetwork are more important over the other edges by minimizing the loss of the subnetwork on their local data). Each client then will send their local edge ranking to the server. Finally, the FRL server uses a novel *voting* mechanism to aggregate client rankings into a global ranking vector, which represents which edges of the random neural network (the supernetwork) will form the global subnetwork.

Intuitions on FRL's robustness: In traditional FL algorithms, clients send large-dimension model updates $\in \mathbb{R}^d$ (real numbers) to the server, providing malicious clients significant flexibility in fabricating malicious updates. By contrast, FRL clients merely share the rankings of the edges of the supernetwork, i.e., integers $\in [1, d]$, where d is the size of the supernetwork. This allows the FRL server to use a voting mechanism to aggregate client updates (i.e., ranks), therefore, providing high resistance to adversarial ranks submitted by poisoning clients, since each client can only cast a single vote! Therefore, as we will show both theoretically and empirically, FRL provides robustness by design and reduces the impact of untargeted poisoning attacks. Furthermore, unlike most existing robust FL frameworks, FRL does not require any knowledge about the percentages of malicious clients.

Intuitions on FRL's communication efficiency: In FRL, the clients and the server communicate just the rankings of the edges in the supernetwork, i.e., a permutation of indices in $[1, d]$. Ranking vectors are generally significantly smaller than the global model. This, as we will show, significantly reduces the upload and download communication in FRL compared to Federated Averaging (FedAvg) [31], where clients communicate model parameters, each of 32/64 bits.

Evaluation results: We experiment with three datasets in real-world heterogeneous FL settings and show that: **(1)** FRL achieves similar performance (e.g., model accuracy) as state-of-the-art FedAvg but with significantly reduced communication costs: for CIFAR10, the accuracy and communication cost per client are 85.4% and 40.2MB for FedAvg, while 85.3% and 26.2MB for FRL. **(2)** FRL is highly robust to poisoning attacks as compared to state-of-the-art robust aggregation algorithms: from 85.4% in the benign setting, 10% malicious clients reduce the accuracy of FL to 56.3% and 58.8% with Trimmed-Mean [45] and Multi-Krum [9], respectively, while FRL's performance only decreases to 79.0%.

We also compare FRL with two communication reduc-

tion methods, SignSGD [7] and TopK [3] and show that FRL produces comparable communication costs and model accuracies. For instance, on CIFAR10, FRL, SignSGD, and TopK achieve 85.3%, 79.1%, and 82.1% test accuracy, respectively, when the corresponding communication costs (download and upload) are 26.2MB, 20.73MB, and 30.79MB. On the other hand, FRL offers significantly superior robustness. For instance, on CIFAR10, 10% (20%) malicious clients reduce the accuracy of SignSGD to 39.7% (10.0%), but FRL's accuracy decreases to only 79.0% (69.5%). TopK is incompatible with existing robust aggregation algorithms, hence uses Average aggregation and is as vulnerable as FedAvg, especially in the real-world heterogeneous settings.

Although our primary focus is on defending against untargeted attacks, we also evaluate the FRL's robustness against targeted poisoning for completeness. We consider state-of-the-art backdoor attacks [4, 42, 44], and we empirically show that FRL is more robust against these backdoor attacks compared to standard weight training FL. For example on CIFAR10, with 2% of malicious clients, semantic backdoor attacks [4] achieve 82.7% (84.4%) average backdoor (clean) task accuracy against FedAvg, while they achieve 49.2% (84.1%) backdoor (clean) task accuracy against FRL.

In summary, we propose a federated learning approach that is built on exchanging rankings instead of parameter weights, and we show a ranking-based FL is more robust to both untargeted and targeted poisoning attacks. Our key contributions are as follows:

- We show that sparsifying the space of FL clients' updates can improve robustness of FL to poisoning. Because, it significantly reduces the space for attackers to search for malicious updates and enables more robust voting-based aggregations. Building on this hypothesis, we design Federated Rank Learning (FRL), a novel FL system in which clients collaboratively train a global model by ranking the importance of the edges of a random network based on their local data.

- We evaluate FRL on three benchmark datasets including MNIST, CIFAR10, FEMNIST where we split them in heterogeneous fashion among a large number of users, i.e., among 1000, 1000, 3400 users respectively. We show that FRL provides more robustness and competitive communication efficiency compared to state-of-the-art AGRs and compression techniques.

- We obtain theoretical robustness bounds for FRL, showing its strong robustness without any knowledge of the number of malicious clients.

2 Related works

Supermask learning: Modern neural networks have a very large number of parameters. These networks are generally overparameterized [16, 17, 27, 28], i.e., they have more parameters than they need to perform a particular task, e.g., classification. The *lottery ticket hypothesis* [19] states that a fully-trained neural network, i.e., *supernetwork*, contains sparse *subnetworks*, i.e., subsets of all neurons in supernetwork, which can be trained from scratch (i.e., by training same initialized weights of the subnetwork) and achieve performances close to the fully trained supernetwork. The lottery ticket hypothesis allows for massive reductions in the sizes of neural networks. Ramanujan et al. [35] offer a complementary conjecture that an overparameterized neural network with randomly initialized weights contains subnetworks which perform as good as the fully trained network.

Poisoning attacks and defenses for federated learning (FL): FL involves mutually untrusting clients. Hence, a *poisoning adversary* may own or compromise some of the FL clients, called *malicious clients*, with the goal of mounting a *targeted* or *untargeted* poisoning attack. In a targeted attack [8, 41], the goal is to reduce the utility of the model on specific test inputs, while in the untargeted attack [5, 18, 33, 38], the goal is to reduce the utility for all (or most) test inputs. It is shown [9] that even a single malicious client can mount an effective untargeted attack on FedAvg.

In order to make FL robust to the presence of such malicious clients, the literature has designed various *robust aggregation rules (AGR)* [9, 13, 32, 45], which aim to remove or attenuate the updates that are more likely to be malicious according to some criterion. For instance, Multi-krum [9] repeatedly removes updates that are far from the geometric median of all the updates, and Trimmed-mean [45] removes the largest and smallest values of each update dimension and calculates the mean of the remaining values. Unfortunately, these robust AGRs are not very effective in non-convex FL settings and multiple works have demonstrated strong targeted [8, 42] and untargeted attacks [18, 38] on them.

Communication cost of FL: In many real-world FL applications, it is essential to minimize the communication between FL server and clients. Especially in cross-device FL, the clients (e.g., mobile phones and wearable devices) have limited resources and communication can be a major bottleneck. There are two major types of communication reduction methods: (1) *Quantization* methods reduce the resolution of (i.e., number of bits used to represent) each dimension of a client update. For instance, SignSGD [7] uses the sign (1 bit) of each dimension of model updates. (2) *Sparsification* methods propose to use only a subset of all the update dimensions. For instance, in TopK [3], only the largest K% update dimensions are sent to the server in each FL round. We note that, communication reduction methods primarily focus on and succeed at reducing upload communication (client → server), but they use the entire model in download communication (server → client).

3 Preliminaries

3.1 Federated learning

In FL [24,25,31], N clients collaborate to train a global model without directly sharing their data. In round t, the service provider (server) selects n out of N total clients and sends them the most recent global model θ^t. Each client trains a local model for E local epochs on their data starting from the θ^t using stochastic gradient descent (SGD). Then the client sends back the calculated gradients (∇_k for kth client) to the server. The server then aggregates the collected gradients and updates the global model for the next round. FL can be either cross-device or cross-silo [24]. In cross-device FL, N is large (from few thousands to billions) and only a small fraction of clients is chosen in each FL training round, i.e., $n \ll N$. By contrast, in cross-silo FL, N is moderate (up to 100) and all clients are chosen in each round, i.e., $n = N$. In this work, we evaluate the performance of FRL and other FL baselines for cross-device FL under realistic production FL settings.

3.2 Edge-popup algorithm

The edge-popup (EP) algorithm [35] is an optimization to find supermasks within a large, randomly initialized neural network, i.e., called *supernetwork*, with performances close to the fully trained supernetwork. EP algorithm does not train the weights (θ^w) of the network, instead only decides the set of edges to keep and removes (pops) the rest of the edges. Specifically, EP algorithm assigns a positive score to each of the edges in the supernetwork (θ^s). On forward pass, it selects top k% edges with highest scores, where k is the percentage of the total number of edges in the supernetwork that will remain in the final subnetwork. On the backward pass, it updates the scores with the straight-through gradient estimator [6].

Algorithm 1 presents EP algorithm. Suppose in a fully connected neural network, there are L layers and layer $\ell \in [1, L]$ has n_ℓ neurons, denoted by $V^\ell = \{V_1^\ell, ..., V_{n_\ell}^\ell\}$. If I_v and Z_v denote the input and output for neuron v respectively, then the input of the node v is the weighted sum of all nodes in previous layer, i.e., $I_v = \sum_{u \in V^{\ell-1}} W_{uv} Z_u$. Here, W_{uv} is the weight of the edge connecting u to v. Edge-popup algorithm tries to find subnetwork E, so the input for neuron v would be: $I_v = \sum_{(u,v) \in E} W_{uv} Z_u$.

Updating scores. Consider an edge E_{uv} that connects two neurons u and v, W_{uv} be the weight of E_{uv}, and s_{uv} be the score assigned to the edge E_{uv} by Edge-popup algorithm. Then the edge-popup algorithm removes edge E_{uv} from the supermask if its score s_{uv} is not high enough. Each iteration of supermask training updates the scores of all edges such that, if having an edge E_{uv} in subnetwork reduces loss (e.g., cross-entropy loss) over training data, the score s_{uv} increases.

Algorithm 1 Edge-popup (EP) algorithm

1: **Input:** number of local epochs E, training data D, initial weights θ^w and scores θ^s, subnetwork size $k\%$, learning rate η
2: **for** $e \in [E]$ **do**
3: $\quad \mathcal{B} \leftarrow$ Split D in B batches
4: $\quad$ **for** batch $b \in [B]$ **do**
5: $\quad\quad$ EP FORWARD $(\theta^w, \theta^s, k, b)$
6: $\quad\quad \theta^s = \theta^s - \eta \nabla \ell(\theta^s; b)$
7: $\quad$ **end for**
8: **end for**
9: **return** θ^s
10: **function** EP FORWARD$(\theta^w, \theta^s, k, b)$
11: $\quad \mathbf{m} \leftarrow$ sort(θ^s)
12: $\quad t \leftarrow$ int$((1-k)*$len$(\mathbf{m}))$
13: $\quad \theta^p = \theta^w \odot \mathbf{m}$, where $\mathbf{m}[:t] = 0$; $\mathbf{m}[t:] = 1$
14: $\quad$ **return** $\theta^p(b)$
15: **end function**

The algorithm selects top k% edges (i.e., finds a subnetwork with sparsity of k%) with highest scores, so I_v reduces to $I_v = \sum_{u \in V^{\ell-1}} W_{uv} Z_u h(s_{uv})$ where $h(.)$ returns 1 if the edge exists in top-k% highest score edges and 0 otherwise. Because of existence of $h(.)$, which is not differentiable, it is impossible to compute the gradient of loss with respect to s_{uv}. Recall that, the Edge-popup algorithm use straight-through gradient estimator [6] to compute gradients. In this approach, $h(.)$ will be treated as the identity in the backward pass meaning that the upstream gradient (i.e., $\frac{\partial L}{\partial I_v}$) goes straight-through $h(.)$. Now using chain rule, we can derive $\frac{\partial L}{\partial I_v} \frac{\partial I_v}{\partial s_{uv}} = \frac{\partial L}{\partial I_v} W_{uv} Z_u$ where L is the loss to minimize. Then we can SGD with step size η to update scores as $s_{uv} \leftarrow s_{uv} - \eta \frac{\partial L}{\partial I_v} Z_u W_{uv}$.

4 Our proposal: Federated Rank Learning

Algorithm 2 Federated Ranking Learning (FRL)

1: **Input:** number of rounds T, number of local epochs E, number of users per round n, seed SEED, learning rate η, subnetwork size $k\%$
2: Server: Initialization
3: $\theta^s, \theta^w \leftarrow$ Initialize random scores and weights using SEED
4: $R_g^1 \leftarrow$ ARGSORT$(\theta^s) \triangleright$ Sort the initial scores and obtain initial rankings
5: **for** $t \in [1, T]$ **do**
6: $\quad U \leftarrow$ set of n randomly selected clients out of N total clients
7: $\quad$ **for** u in U **do**
8: $\quad\quad$ Clients: Calculating the ranks
9: $\quad\quad \theta^s, \theta^w \leftarrow$ Initialize scores and weights using SEED
10: $\quad\quad \theta^s[R_g^t] \leftarrow$ SORT$(\theta^s) \triangleright$ sort the scores based on the global ranking
11: $\quad\quad S \leftarrow$ Edge-PopUp$(E, D_u^{tr}, \theta^w, \theta^s, k, \eta) \quad \triangleright$ Client u uses Algorithm 1 to train a supermask on its local training data
12: $\quad\quad R_u^t \leftarrow$ ARGSORT$(S) \quad\quad \triangleright$ Ranking of the client
13: $\quad$ **end for**
14: $\quad$ Server: Majority Vote
15: $\quad R_g^{t+1} \leftarrow$ VOTE$(R_{\{u \in U\}}^t) \quad\quad \triangleright$ Majority vote aggregation
16: **end for**
17: **function** VOTE$(R_{\{u \in U\}})$:
18: $\quad V \leftarrow$ SUM(ARGSORT$(R_{\{u \in U\}})$), $A \leftarrow$ SUM(V)
19: $\quad$ **return** ARGSORT(A)
20: **end function**

In this section, we provide the design of our *federated*

rank learning (FRL) algorithm (Algorithm 2). FRL clients collaborate (without sharing their data) to *find a subnetwork* within a *randomly initialized, untrained supernetwork*, with scores θ^s and weights θ^w. In each round, FRL first finds a unanimous (global) ranking of the supernetwork edges and then uses the subnetwork of the top ranked edges as the global model.

The objective of FRL is to find a global ranking R_g and convert it to a global binary mask, $\mathbf{m}$, such that resulting subnetwork, $\theta^w \odot \mathbf{m}$, minimizes the average loss of all clients. FRL optimization can be formalized as follows:

$$\min_{R_g} F(\theta^w, R_g) = \min_{R_g} \sum_{i=1}^{N} \lambda_i L_i(\theta^w \odot \mathbf{m}) \qquad (1)$$

$$\text{s.t. } \mathbf{m}[R_g < k] = 0 \text{ and } \mathbf{m}[R_g \geq k] = 1$$

where N is the total number of FRL clients, L_i is the loss function for the ith client, λ_i is the importance, e.g., weight, of the ith client; we use $\lambda_i = \frac{1}{N}$, i.e., all clients have the same weight. $\mathbf{m}$ is the final binary mask, where edges with top k ranks (layer-wise) get '1' while others get '0'. We use $\mathbf{m}$ to compute final global model by superimposing $\mathbf{m}$ on θ, i.e., the we use the subnetwork $\theta \odot \mathbf{m}$ as the final global model. In Figure 2, we demonstrate a single FRL round using a supernetwork with six edges $e_{i \in [0,5]}$ and three clients $C_{j \in [1,3]}$ who aim to find a subnetwork of size $k=50\%$ of the original supernetwork.

4.1 Server: Initialization (only for round $t = 1$)

In the first round, the FRL server chooses a random seed SEED to generate initial random weights θ^w and scores θ^s for the global supernetwork θ; note that, θ^w, θ^s, and SEED remain constant during the entire FRL training. Next, the FRL server shares SEED with FRL clients, who can then locally reconstruct the initial weights θ^w and scores θ^s using SEED. Figure 2-① depicts this step.

Recall that, the goal of FRL training is to find the most important edges in θ^w without changing the weights. Unless specified otherwise, both server and clients use the Signed Kaiming Constant algorithm [35] to generate random weights and the Kaiming Uniform algorithm [21] to generate random scores. However, in Section 7.5.2, we also explore the impacts of different weight initialization algorithms on the performance of FRL. We use the same seed to initialize weights and scores.

At the beginning, the FRL server finds the global rankings of the initial random scores (Algorithm 2 line 4), i.e., $R_g^1 = \text{ARGSORT}(\theta^s)$. We define *rankings of a vector* as the indices of elements of vector when the vector is sorted from low to high, which is computed using ARGSORT function.
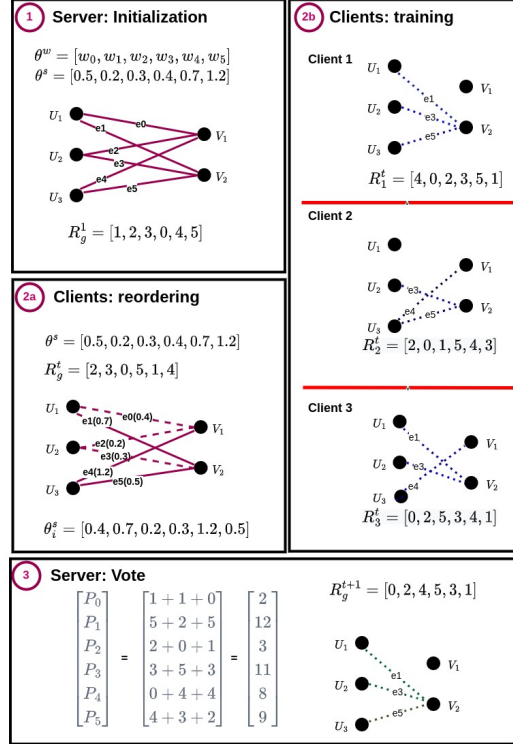

Figure 2: A single FRL round with three clients and supernetwork of 6 edges.

4.2 Clients: Calculating the ranks (for each round t)

In the tth round, FRL server randomly selects n clients among total N clients, and shares the global rankings R_g^t with them. Each of the selected n clients locally reconstructs the weights θ^w's and scores θ^s's using SEED (Algorithm 2 line 9). Then, each FRL client reorders the random scores based on the global rankings, R_g^t (Algorithm 2 line 10); we depict this in Figure 2-②a.

Next, each of the n clients uses reordered θ^s and finds a subnetwork within θ^w using Algorithm 1; to find a subnetwork, they use their local data and E local epochs (Algorithm 2 line 11). Note that, each iteration of Algorithm 1 updates the scores S starting from θ^s. Then client u computes their local rankings R_u^t using the final updated scores (S) and ARGSORT(.), and sends R_u^t to the server. Figure 2-②a shows how each of the selected n clients reorders the random scores using global rankings. For instance, the initial global rankings for this round are $R_g^t = [2, 3, 0, 5, 1, 4]$, meaning that edge e_4 should get the highest score ($s_4 = 1.2$), and edge e_2 should get the lowest score ($s_2 = 0.2$).

Figure 2-②b shows, for each client, the scores and rankings they obtained after finding their local subnetwork. For example, rankings of client C_1 are $R_1^t = [4, 0, 2, 3, 5, 1]$, i.e., e_4 is the least important and e_1 is the most important edge for C_1. Considering desired subnetwork size to be 50%, C_1 uses

edges {3,5,1} in their final subnetwork.

4.3 Server: Majority vote (for each round t)

The server receives all the local rankings of the selected n clients, i.e., $R^t_{\{u \in U\}}$. Then, it performs a majority vote over all the local rankings using VOTE(.) function. Note that, for client u, the index i represents the importance of the edge $R^t_u[i]$ for C_u. For instance, in Figure 2-②b, rankings of C_1 are $R^t_1 = [4,0,2,3,5,1]$, hence the edge e_4 at index=0 is the least important edge for C_1, while the edge e_1 at index=5 is the most important edge. Consequently, VOTE(.) function assigns reputation=0 to edge e_4, reputation=1 to e_0, reputation=2 to e_2, and so on. In other words, for rankings R^t_u of C_u and edge e_i, VOTE(.) computes the reputation of e_i as its index in R^t_u. Finally, VOTE(.) computes the total reputation of e_i as the sum of reputations from each of the local rankings. In Figure 2-②b, reputations of e_0 are 1 in R^t_1, 1 in R^t_2, and 0 in R^t_3, hence, the total reputation of e_0 is 2. We depict this in Figure 2-③; here, the final total reputations for edges $e_{\{i \in [0,5]\}}$ are $A = [2,12,3,11,8,9]$. Finally, the server computes global rankings R^{t+1}_g to use for round $t+1$ by sorting the final total reputations of all edges, i.e., $R^{t+1}_g = \text{ARGSORT}(A)$.

Note that, *all FRL operations that involve sorting, reordering, and voting are performed in a layer-wise manner*. For instance, the server computes global rankings R^t_g in round t for each layer separately, and consequently, the clients selected in round t reorder their local randomly generated scores θ^s for each layer separately.

5 Robustness of FRL to poisoning

FRL and FL are distributed learning algorithms with mutually untrusting clients. Hence, a *poisoning adversary* may own or compromise some of FRL (FL) clients, called *malicious clients*, and mount a *targeted* or *untargeted* poisoning attack. As discussed in Section 1, we mainly focus on the more severe untargeted attacks and show that FRL is significantly more robust by design to such poisoning attacks. However, for completeness we also evaluate robustness of FRL against targeted attacks in Appendix C.

Intuition behind robustness of FRL: Existing FL algorithms, including robust algorithms, are shown to be vulnerable to various poisoning attacks [39]. One of the key reasons behind the susceptibility of existing algorithms is that their model updates can have a large continuous space of values. For instance, to manipulate vanilla FedAvg, malicious clients send very large updates [9], and to manipulate Multi-krum and Trimmed-mean, [18, 38] propose to perturb a benign update in a specific malicious direction. On the other hand, in FRL, clients must send a permutation of indices $\in [1, n_\ell]$ for each layer. Hence, FRL significantly reduces the space of the possible malicious updates that an adversary can craft. Major-

ity voting in FRL further reduces the chances of successful attack. Intuitively, this makes FRL design robust to poisoning attacks. Below, we make this intuition more concrete.

The worst-case untargeted poisoning attack on FRL: Here, the poisoning adversary aims to reduce the accuracy of the final global FRL subnetwork on most test inputs. To achieve this, the adversary should replace the high ranked edges with low ranked edges in the final subnetwork. For the worst-case analysis of FRL, we assume a very strong adversary (i.e., threat model): 1) each of the malicious clients has some data from benign distribution; 2) malicious clients know the entire FRL algorithm and its parameters; 3) malicious clients can collude. Under this threat model we design a worst case attack on FRL (Algorithm 3), which executes as follows: First, malicious clients compute rankings on their benign data and use VOTE(.) algorithm to compute an aggregate rankings. Finally, each of the malicious clients uses the reverse of the aggregate rankings to share with the FRL server in given round. The adversary should invert the rankings layer-wise as the FRL server will aggregate the local rankings per layer too, and it is not possible to mount a model-wise attack.

Algorithm 3 FRL Poisoning

1: **Input:** number of malicious clients M, number of malicious local epochs E', seed SEED, global ranking R^t_g, learning rate η, subnetwork size $k\%$
2: **function** MALICIOUSUPDATE(M, SEED, R^t_g, E', η, k):
3:     **for** $mu \in [M]$ **do**
4:         Malicious Client Executes:
5:         $\theta^s, \theta^w \leftarrow$ Initialize random scores and weights using SEED
6:         $\theta^s[R^t_g] \leftarrow \text{SORT}(\theta^s)$
7:         $S \leftarrow$ Edge-PopUp($E', D^{tr}_u, \theta^w, \theta^s, k, \eta$)
8:         $R^t_{mu} \leftarrow \text{ARGSORT}(S)$ ▷ Ranking of the malicious client
9:     **end for**
10:     Aggregation:
11:     $R^t_m \leftarrow \text{VOTE}(R^t_{\{mu \in [M]\}})$ ▷ Majority vote aggregation
12:     **return** REVERSE(R^t_m)   ▷ reverse the ranking
13: **end function**

Now we justify why the attack in Algorithm 3 is the worst case attack on FRL for the strong threat model. Note that, FRL aggregation, i.e., VOTE(.), computes the reputations using clients' rankings and sums the reputations of each network edge. Therefore, the strongest poisoning attack would want to reduce the reputation of good edges. This can be achieved following the aforementioned procedure of Algorithm 3 to reverse the rankings computed using benign data.

Theoretical analysis of robustness of FRL algorithm: In this section, we prove an upper bound on the failure probability of robustness of FRL, i.e., the probability that a good edge will be removed from the final subnetwork when malicious clients mount the worst case attack.

Following the work of [7], we make two assumptions in order to facilitate a concrete robustness analysis of FRL: a) each malicious client has access only to its own data, and b) we consider a simpler VOTE(.) function, where the FRL server puts an edge e_i in the final subnetwork if more than half of

the clients have e_i (a good edge) in their local subnetworks. In other words, the rankings that each client sends to the server is just a bit mask showing that each edge should or should not be in the final subnetwork. The server makes a majority vote on the bit masks, and if an edge has more than half votes, it will be in the global subnetwork. Our VOTE(.) mechanism has more strict robustness criterion, as it uses more nuanced reputations of edges instead of bit masks. Hence, the upper bound on failure probability in this section also applies to the FRL VOTE(.) function.

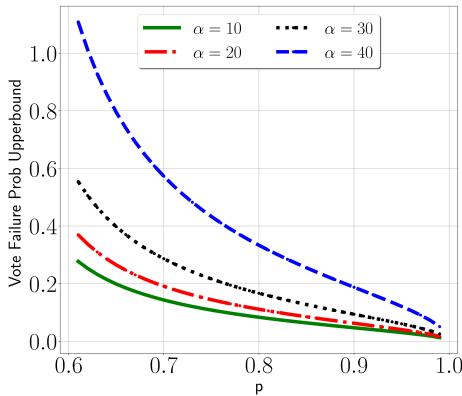Figure 3: Upper bound on the failure probability of VOTE(.) function in FRL. α is the percentages of malicious clients and p is the probability that a benign client puts a good edge in its top k ranks.

The probability that our voting system fails is the probability that more than half of the votes do not include e_i in their subnetworks. The upper bound on the probability of failure would be $1/2\sqrt{\frac{np(1-p)}{(n(p+\alpha(1-2p)-1/2))^2}}$, where n is the number of clients being processed, p is the probability that a benign client puts e_i in their top ranks, and α is the fraction of malicious clients. We defer the detailed proof to Appendix A. Figure 3 shows the upper bound on the failure of VOTE(.) for different values of α and p. As can be seen, the higher the probability p, the higher the robustness of FRL.

6 Communication efficiency of FRL

In FL, and especially in the cross-device setting, clients have limited communication bandwidth. Hence, FL algorithms must be communication efficient. We discuss here the communication cost of FRL algorithm. In the first round, the FRL server only sends one seed of 32 bits to all the FRL clients, so they can construct the random weights (θ^w) and scores (θ^s). In a round t, each of selected FRL clients receives the global rankings R_g^t and sends back their local rankings R_u^t. The rankings are a permutation of the indices of the edges in each layer, i.e., of $[0, n_\ell - 1] \forall \ell \in [L]$ where L is the number of layers and n_ℓ is the number of parameters in ℓth layer.
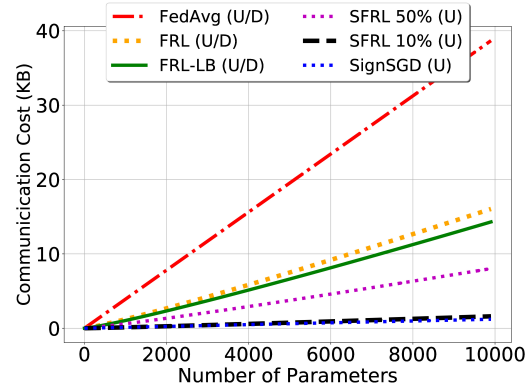

Figure 4: Upload (U) and download (D) Communication cost analysis. The download cost (D) of all SFRLs would be the same as FRL. Download communication cost of SignSGD would be the same as FedAvg too.

We use the naive approach to communicate layer-wise rankings, where each FRL client exchanges a total of $\sum_{\ell \in [L]} n_\ell \times \log(n_\ell)$ bits. Because, for the layer ℓ, the client receives and sends n_ℓ ranks where each one is encoded with $\log(n_\ell)$ bits. On the other hand, a client exchanges $\sum_{\ell \in [L]} n_\ell \times 32$ bits in FedAvg, when 32 bits are used to represent each of n_ℓ weights in layer ℓ. In Section 7.3, we measure the performance and communication cost of FRL with other existing FL compressors SignSGD [7] and TopK [2, 3].

Sparse-FRL: Here, we propose Sparse-FRL, a simple extension of FRL to further reduce the communication cost. In Sparse-FRL, a client sends only the most important ranks of their local rankings to the server for aggregation. For instance, in Figure 2, client C_1 sends $R_1^t = [4, 0, 2, 3, 5, 1]$ in case of FRL. But in sparse-FRL, with sparsity set to 50%, client C_1 sends just the top 3 rankings, i.e., sends $R_1''^t = [3, 5, 1]$. For each client, the sparse-FRL server assumes 0 reputation for all of the edges not included in the client's rankings, i.e., in Figure 2, sparse-FRL server will assign reputation=0 for edges e_4, e_0, and e_2. Then the server uses VOTE(.) to compute total reputations of all edges and then sort them to obtain the final aggregate global rankings, i.e., R_g^{t+1}, to use for subsequent rounds. We observe in out experiments, that sparse-FRL performs very close to FRL, even with sparsity as low as 10%, while also significantly reducing the communication cost.

Lower-bound of communication cost of FRL: Since the FRL clients send and receive layer-wise rankings of indices, i.e., integers $\in [0, n_\ell - 1]$, for layer ℓ, there are $n_\ell!$ possible permutations for layer $\ell \in [L]$. If we use the best possible compression method in FRL, an FRL client needs to send and receive $\sum_{\ell \in [L]} \log(n_\ell!)$ bits. Therefore, the download and upload bandwidth for each FRL client would be $\sum_{\ell \in [L]} \log(n_\ell * (n_\ell - 1) * ... * 2 * 1) = \sum_{\ell \in [L]} \sum_{i=1}^{n_\ell} log(i)$ bits. Please note that in our experiment, FRL clients send and receive the rankings without any further compression, and

$\sum_{\ell \in [L]} \sum_{i=1}^{n_\ell} log(i)$ just shows a lower-bound of communication cost of FRL.

In Figure 4, we compare the upload and download communication costs of one client per FL round for FedAvg, SignSGD, and different variants of FRL for different number of parameters. U and D are showing upload and download communication cost. Please note that the download communication cost of all SFRLs would be the same as FRL, and download communication cost of SignSGD would be similar to FedAvg too. If we use a compression method to compress the local rankings (for upload) and global rankings (for download), we can improve communication cost of FRL to its lower-bound (FRL-LB in Figure 4). In this Figure, we can see that SFRL can provide competitive upload communication cost and lower download communication cost compared to SignSGD when the clients are sending only 10% of top local rankings (SFRL 10%).

7 Empirical evaluation

In this section, we extensively evaluate the utility, robustness, and communication cost of our FRL algorithm. This section is organized as follows: in Section 7.1 we discuss the experimental setup. In Section 7.2 we investigate the robustness and utility of FRL, followed by Section 7.3 in which we discuss the communication cost of FRL. Next, in Section 7.4, we compare FRL utility and robustness to an extension of edge-popup to FL. We conclude with Section 7.5, where we provide an ablation study on FRL. We have released the code for reproducibility. [2]

7.1 Experimental setup

7.1.1 Datasets and their distribution

We use MNIST, CIFAR10, and FEMNIST datasets. Most real-world FL settings have heterogeneous client data, hence following previous works [22, 37], we distribute MNIST and CIFAR10 datasets among 1,000 clients in non-iid fashion using *Dirichlet* distribution with parameter $\beta = 1$. Note that, increasing β results in more iid datasets. FEMNIST is naturally distributed non-iid among 3,400 clients. We further split the datasets of each client into training (80%) and test (20%).

We run all the experiments for 2000 global rounds of FRL and FL, while selecting 25 clients in each round. At the end of the training, we calculate the test accuracy of all the clients on the final global model, and we report the mean and standard deviation of all clients' test accuracies in our experiments. Due to space restrictions, we defer further details of datasets, model architectures, and corresponding hyperparameters settings to Appendix B.1. We independently tune the hyperparameters for FRL and other baselines (Section 7.1.2).

We also evaluate the utility of FRL on a significantly more complicated task, Tiny-ImageNet [1] in Section 7.5.4.

7.1.2 Baseline FL algorithms

We compare the FRL with following FL baselines:

Federated averaging: In non-adversarial FL settings, i.e., without any malicious clients, the dimension-wise Average (FedAvg) [25, 31] is an effective AGR. In fact, due to its efficiency, Average is the only AGR implemented by FL applications in practice [30, 34].

SignSGD: is a quantization method used in distributed learning to compress each dimension of gradient updates into 1 bit instead of 32 or 64 bits. To achieve this, in SignSGD [7] the clients only send the sign of their gradient updates to the server, and the server runs a majority vote on them. SignSGD is designed for distributed learning where all the clients participate in each round, so all the clients are aware of the most updated weight parameters of the global model. However, SignSGD only reduces upload communication (clients→server). But, does not reduce download communication (server→clients), i.e., to achieve good performance of the global model, the server sends all the weight parameters (each of 32 bits) to the newly selected clients in each round. Hence, SignSGD is as inefficient as FedAvg in download communication.

TopK: is a sparsification method used in distributed learning that transmits only a few dimensions of each model update to the server. In TopK [2, 3], the clients first sort the absolute values of their local model updates, and send the Top K% largest model update dimensions to the server for aggregation. TopK suffers from the same problem as SignSGD: for performance reasons, the server should send the entire updated model weights to the new selected clients.

Multi-krum: [9] proposed Multi-krum AGR as a modification to their own Krum AGR. Multi-krum selects an update using Krum and adds it to a selection set, S. Multi-krum repeats this for the remaining updates (which remain after removing the update that Krum selects) until S has c updates such that $n - c > 2m + 2$, where n is the number of selected clients and m is the number of compromised clients in a given round. Finally, Multi-krum averages the updates in S.

Trimmed-mean: Yin et al. [45] proposed Trimmed-mean that aggregates each dimension of input updates separately. It sorts the values of the jth-dimension of all updates. Then it removes m (i.e., the number of compromised clients) of the largest and smallest values of that dimension, and computes the average of the rest of the values as its aggregate for the dimension j.

7.2 Analyses of robustness to poisoning

We compare FRL with state-of-the-art robust aggregation rules (AGRs): Mkrum [9], and Trimmed-mean [45]. Table 1

Table 1: Comparing the robustness of various FL algorithms: FRL and Sparse-FRL (SFRL) (in **bold**) outperform the state-of-the-art robust AGRs and SignSGD against the strongest of untargeted poisoning attacks.

Dataset	AGR	No malicious	10% malicious	20% malicious
MNIST + LeNet 1000 clients	FedAvg	98.8 (3.2)	10.0 (10.0)	10.0 (10.0)
	Trimmed-mean	98.8 (3.2)	95.1 (7.7)	87.6 (9.5)
	Multi-krum	98.8 (3.2)	98.6 (3.3)	97.9 (4.1)
	SignSGD	97.2 (4.6)	96.6 (5.0)	96.2 (5.6)
	FRL	**98.8 (3.1)**	**98.8 (3.1)**	**98.7 (3.3)**
	SFRL Top 50%	**98.2 (3.8)**	**97.04 (4.4)**	**95.1 (7.8)**
CIFAR10 + Conv8 1000 clients	FedAvg	85.4 (11.2)	10.0 (10.1)	10.0 (10.1)
	Trimmed-mean	84.9 (11.0)	56.3 (16.0)	20.5 (13.2)
	Multi-krum	84.7 (11.3)	58.8 (15.8)	25.6 (14.4)
	SignSGD	79.1 (12.8)	39.7 (15.9)	10.0 (10.1)
	FRL	**85.3 (11.3)**	**79.0 (12.4)**	**69.5 (14.8)**
	SFRL Top 50%	**77.6 (13.0)**	**41.7 (15.4)**	**39.7 (15.2)**
FEMNIST + LeNet 3400 clients	FedAvg	85.8 (10.2)	6.3 (5.8)	6.3 (5.8)
	Trimmed-mean	85.2 (11.0)	72.7 (15.7)	56.2 (20.3)
	Multi-krum	85.2 (10.9)	80.9 (12.2)	23.7 (12.8)
	SignSGD	79.3 (12.4)	76.7 (13.2)	55.1 (14.9)
	FRL	**84.2 (10.7)**	**83.0 (10.9)**	**65.8 (17.8)**
	SFRL Top 50%	**75.2 (12.7)**	**70.5 (14.4)**	**60.39 (14.8)**

gives the performances of robust AGRs, SignSGD, and FRL with different percentages of malicious clients using attacks proposed by Shejwalkar et al. [38], Bernstein et al. [7], and Algorithm 3 respectively. To attack FRL, we choose 25 random malicious clients in each FRL round to generate the malicious update. Here, we make a rather impractical assumption in favor of the *previous* robust AGRs: we assume that the server knows the exact % of malicious clients in each FL round. Note that, *FRL does not require this knowledge.*

FRL achieves higher robustness than state-of-the-art robust AGRs: We note from Table 1 that, FRL is more robust to the presence of malicious clients who mount untargeted poisoning attacks, compared to Multi-Krum and Trimmed-mean, when percentages of malicious clients are 10% and 20%. For instance, on CIFAR10, 10% malicious clients can decrease the accuracy of FL models to 56.3% and 58.8% for Trimmed-mean and Multi-Krum respectively; 20% malicious clients can decrease the accuracy of the FL models to 20.5% and 25.6% for Trimmed-mean and Multi-Krum respectively. On the other hand, FRL performance decreases to 79.0% and 69.5% for 10% and 20% attacking ratio, respectively.

We make similar observations for MNIST and FEMNIST datasets: for FEMNIST, 10% (20%) malicious clients reduce accuracy of the global model from 85.8% to 72.7% (56.2%) for Trimmed-Mean, and to 80.9% (23.7%) for Multi-krum, while FRL accuracy decreases to 83.0% (65.8%).

FRL is more accurate than SignSGD: First, we note that, in the absence of malicious clients, FRL is significantly more accurate than SignSGD. For instance, on CIFAR10 distributed in non-iid fashion among 1000 clients, FRL achieves 85.3% while SignSGD achieves 79.1% , or on FEMNIST, FRL achieves 84.2% while SignSGD achieves 79.3%. This is because, FRL clients send more nuanced information via rankings of their subnetworks compared to SignSGD, where clients just send the signs of their model updates.

FRL is more robust than SignSGD: Next, we note from Table 1 that, FRL is more robust against untargeted poisoning attacks compared to SignSGD when percentages of malicious clients are 10% and 20%. For instance, on CIFAR10, 10% (20%) malicious clients can decrease the accuracy of SignSGD model to 39.8% (10.0%). On the other hand, FRL performance decreases to 79.0% and 69.5% for 10% and 20% attacking ratio respectively. We make similar observations for MNIST and FEMNIST datasets: for FEMNIST, 10% (20%) malicious clients reduce accuracy of the global model from 85.8% to 76.7% (55.1%) for SignSGD, while FRL accuracy decreases to 83.0% (65.8%).

Sparse-FRL robustness: We evaluate robustness of SFRL Top 50% against 10% and 20% malicious clients. As we can see from Table 1, by sending only top half of the local rankings, the accuracy goes from 85.3% (FRL) to 77.6% (SFRL). SFRL also can provide robustness to some extend, but adversary has more influence on the global ranking since half of the rankings are missing. For instance, on CIFAR10, 10% (20%) malicious clients can decrease the accuracy of global ranking to 41.7% (39.7%) from 77.6%. Also for FEMNIST, 10% (20%) malicious clients can decrease the accuracy of global ranking to 70.5% (60.39%) from 75.2%. We can see when malicious clients' percentages are higher, SFRL can perform better compared to existing robust AGR.

Table 2: Comparing the accuracy and communication cost of FedAvg, SignSGD, TopK, FRL and Sparse-FRL (SFRL) with different percentages of sparsity (in **bold**). Parentheses in the accuracy column show standard deviation of the accuracy.

Algorithm	Accuracy	Upload/Download (MB)
MNIST + LeNet + 1000 clients		
FedAvg	98.8 (3.1)	6.20/ 6.20
FRL	**98.8 (3.2)**	**4.05/ 4.05**
SFRL Top 50%	**98.2 (3.8)**	**2.03/ 4.05**
SFRL Top 10%	**89.5 (9.2)**	**0.40/ 4.05**
SignSGD	97.2 (4.6)	0.19/ 6.20
TopK 50%	98.8 (3.2)	3.29/ 6.20
TopK 10%	98.7 (3.2)	0.81/ 6.20
CIFAR10 + Conv8 + 1000 clients		
FedAvg	85.4 (11.2)	20.1/ 20.1
FRL	**85.3 (11.3)**	**13.1/ 13.1**
SFRL Top 50%	**77.6 (13.0)**	**6.5/ 13.1**
SFRL Top 10%	**27.5 (14.4)**	**1.3/ 13.1**
SignSGD	79.1 (13.6)	0.63/ 20.1
TopK 50%	82.1 (11.8)	10.69/ 20.1
TopK 10%	77.8 (13.0)	2.64/ 20.1
FEMNIST + LeNet + 3400 clients		
FedAvg	85.8 (10.2)	6.23/ 6.23
FRL	**84.2 (10.7)**	**4.06/ 4.06**
SFRL Top 50%	**75.2 (12.7)**	**2.03/ 4.06**
SFRL Top 10%	**59.2 (15.0)**	**0.40/ 4.06**
SignSGD	79.3 (12.4)	0.19/ 6.23
TopK 50%	85.7 (9.9)	3.31/ 6.23
TopK 10%	85.5 (10.0)	0.81/ 6.23

FRL versus FedAvg and TopK: We omit the results of non-robust aggregations, FedAvg and TopK, because even a single malicious client [9] can jeopardize their performances.

Robustness of FRL against targeted poisoning: Although our primary focus is on defending against untargeted attacks, for completeness, we also evaluate the FRL's robustness against targeted poisoning, and especially against state-of-the-art backdoor attacks [4, 42, 44] in Appendix C. Backdoor attacks are successful in traditional continuous updates based FL (e.g., FedAvg), because in a given round, the adversary can scale its malicious update and cancel the effect of benign clients' updates, thereby forcing the global model to be their malicious model [4]. However, by design, FRL is robust to such scaling as it uses rankings based updates where scaling is impossible.

However, we empirically show that FRL is more robust than tradition FL algorithms, even against the backdoor attacks that do not use scaling [4, 42]. For example, with 2% of malicious clients and non-iid distributed CIFAR10 data, semantic backdoor attacks [4] achieve **82.7%** (84.4%) average backdoor (clean) task accuracy against FedAvg, while they achieve **49.2%** (84.1%) backdoor (clean) task accuracy against FRL.

7.3 Communication cost analysis

In FRL, both clients and server communicate just the edge ranks instead of weight parameters. Thus, FRL reduces both

upload and download communication cost. Table 2 illustrates the utility, i.e., the mean and standard deviation of all clients' test accuracies and, communication cost of FRL and state-of-the-art quantization (i.e., SignSGD [7]) and sparsification (i.e., TopK [2, 3]) communication-reduction methods.

FRL versus SignSGD: SignSGD in FL reduces only the upload communication, but for efficiency reasons, the server sends all of the weight parameters (each of 32 bits) to the newly selected clients. Hence, SignSGD has very efficient upload communication, but very inefficient download communication. For instance, on CIFAR10, for both upload and download, FRL achieves 13.1MB each while SignSGD achieves 0.63MB and 20.1MB, respectively.

FRL versus TopK: We compare FRL and TopK where $K \in \{10, 50\}$%. FRL is more accurate than Topk for MNIST and CIFAR10: on CIFAR10, FRL accuracy is 85.3%, while TopK accuracies are 82.1% and 77.8% with K=50% and K=10%, respectively. Similar to SignSGD, Topk more efficiently reduces upload communication, but has very high download communication. Therefore, the combined upload and download communication cost per client per round is 26.2MB for FRL and 30.79MB for TopK with K=50%; note that, even then TopK performs worse than FRL.

Communication cost reduction due to Sparse-FRL (SFRL): We now evaluate SFRL explained in Section 6. In SFRL with top 50% ranks, clients send the top 50% of their ranks to the server, which reduces the upload bandwidth consumption by half. Please note that the download cost of SFRL is the same as FRL since the FRL server should send all the global rankings to the selected clients in each round. We note from Table 2 that, by sending fewer ranks, SFRL reduces upload communication at a small cost of performance. For instance, on CIFAR10, SFFRL with top 50% reduces the upload communication by 50% at the cost reducing accuracy from 85.4% to 77.6%.

7.4 Comparison with naïve extension of edge-popup algorithm to FL

As discussed in Section 4.2, prior works [36] on supermask training and its following works [14, 43] do not consider rankings, and instead find subnetworks in randomly initialized networks by just training the scores, in a centralized training setting. Algorithm 4 shows the naïve extension of [36] to FL, where the clients train and exchange scores (32bits floats). Like FedAvg, these scores are from a continuous space of float numbers (as opposed to parameter ranks in FRL). At the end of each FL round, the server averages the local score updates to aggregate them and produces global scores (different from our majority vote aggregation). It is important to note that our majority vote aggregation only works on a set of ranking inputs.

Exchanging such scores is as vulnerable to poisoning as regular FL because they are not scale-free and discrete similar

Algorithm 4 Edge-popup based FL (EFL)

1: **Input:** number of rounds T, number of local epochs E, number of users in each round n, seed SEED, learning rate η, subnetwork size $k\%$
2:   Server: Initialization
3:   $\theta_0^s, \theta^w \leftarrow$ Initialize random scores and weights using SEED
4: **for** $t \in [1, T]$ **do**
5:     $U \leftarrow$ set of n randomly selected clients out of N total clients
6:     **for** u in U **do**
7:         Clients: Calculating the scores using EP
8:         $\theta^w \leftarrow$ Initialize weights using SEED
9:         $S_u^t \leftarrow$ Edge-PopUp$(E, D_u^{tr}, \theta^w, \theta_{t-1}^s, k, \eta)$ ▷ Client u uses Algorithm1 to train a supermask starting from global scores θ_{t-1}^s
10:     **end for**
11:     Server: Averaging the scores
12:     $\theta_{t+1}^s \leftarrow$ AVG$(S_{\{u \in U\}}^t)$
13: **end for**

to rankings. Table 3 compares the performance of FedAvg, where the clients train weight parameters, EdgePopUPFL, using this naïve application of Edge-popup where the clients train scores, and FRL, where the clients are training rankings. If we use scores as the clients' updates, even one malicious client can generate its adversarial score update and re-scales it to cancel the effect of other benign updates. On the other hand, rankings are scale-free, and the adversary cannot increase its influence by re-scaling the rankings.

Table 3: Comparing the robustness of EFL, a naïve edge-popup based FL (Algorithm 4), with robustness of FRL.

Dataset # of clients	AGR	Percentage of Malicious Clients		
		0%	10%	20%
CIFAR10 + Conv8 **1000 clients**	FedAvg	85.4 (11.2)	10.0 (10.1)	
	EFL	84.2 (11.3)	10.0 (10.1)	
	FRL	**85.3 (11.3)**	**79.0 (12.4)**	**69.5 (14.8)**

Furthermore, as discussed in Section 4, FRL's performance does not just come from using the Edge-popup algorithm, but rather from introducing an efficient protocol to rank and aggregate them which enables achieving high accuracy and robustness. Overall, a major novelty of our work is that, to the best of our knowledge, FRL is the first scalable, distributed training algorithm that trains using parameters rankings to effectively defend against poisoning attacks. Below is the summary of our contributions compared to the naïve extension of [36] to FL:

- Transform the continuous, local scores into discrete and scale-free rankings (Section 4.2).
- Develop algorithms to aggregate local rankings to produce global rankings (Section 4.3).
- Map global rankings back to local scores for further local training (Section 4.2).

7.5 Ablation study

In this section, we perform an extensive ablation study to understand performances of FRL under various settings. Specifically, we evaluate the performances of FRL while varying

Table 4: Comparing the performance of FRL and FedAvg in cross-device FL setting using two non-iid data distribution methods. We distribute data among 1000 clients with two methods described briefly below; please check Section 7.5.1 for more details.

Dataset	Type of Non-IID	Metric	Algorithm	
			FedAvg	FRL
MNIST LeNet N=1000	Dirichlet Distribution $\beta = 1$	Mean	98.8	98.8
		STD	3.1	3.1
		Min	75.0	75.0
		Max	100	100
	Randomly 2 classes assigned to each client	Mean	98.4	98.3
		STD	4.3	4.1
		Min	70.0	80.0
		Max	100	100
CIFAR10 Conv8 N=1000	Dirichlet Distribution $\beta = 1$	Mean	85.4	85.3
		STD	11.2	11.3
		Min	33.3	33.3
		Max	100	100
	Randomly 2 classes (assigned to each client)	Mean	70.6	70.9
		STD	21.9	19.2
		Min	0	10.0
		Max	100	100

non-iid data distributions methods (Section 7.5.1), weight initialization algorithms (Section 7.5.2), sparsity (Section 7.5.3), and size of supernetwork (Section 7.5.4).

7.5.1 FRL under different heterogeneous data distribution methods

So far, we evaluated all of our experiments when the data is distributed non-iid using Dirichlet distribution with parameter $\beta = 1$. In this method of non-iid data distribution, all clients will get at least a few samples from each data class with non-zero probabilities that Dirichlet distribution generates. However, this non-iid data distribution need not represent all the practical FL settings. In fact, there may exist non-iid distributions that make training FL models more difficult. Therefore in this section, we consider a more difficult setting where the data distribution is more non-iid.

Assigning only two classes to each client: We experiment with the more extreme non-iid distribution considered by McMahan et al. [31]. More specifically, to distribute of MNIST and CIFAR10 data among 1000 clients, we sort all the (i.e., combined train and test) MNIST and CIFAR10 data according to their classes and then we partition them into 2000 shards. Hence, each shards of training MNIST has 30 images and each CIFAR10 shard has 25 images of a single class. Then we assign two random shards to each client resulting in each client having data from at most two classes. Therefore, in CIFAR10 experiments, each client has 50 training images, and 10 test images, and in MNIST experiments, each client has 60 training images and 10 test images. We only use this assignment in Section 7.5.1.

Table 4 shows the performances of FRL and FedAvg using

different methods of non-iid assignment. We distribute the data between 1000 clients using: (I) Dirichlet distribution with $\beta = 1$ similar to [22, 37] and (II) the method described above from [31]. In Table 4, we note that *FRL achieves similar performances as FedAvg for different heterogeneous data distribution methods*. For instance, on CIFAR10, FedAvg and FRL achieves similar performances of 85.4% and 85.3% respectively when data is distributed according to (I). Similarly, when data is distributed according to (II), FedAvg and FRL achieve similar performances of 70.6% and 70.9%, respectively.

We make similar observations for MNIST as well: FedAvg achieves 98.8% and 98.4% for the two methods of data distribution respectively, while FRL achieves 98.8% and 98.3% accuracy.

7.5.2 FRL under different weight initializations

Table 5: Comparing the performance of FRL with different random weight initialization algorithms with the performance of vanilla FedAvg for cross-device setting. Using Singed Kaiming Constant (U_K) as weight initialization gives the best performance for all the datasets.

Dataset	Metric	Algorithm			
		FedAvg	FRL		
	$W_{init} \sim$	-	$\mathcal{X}_N$	$\mathcal{N}_K$	U_K
MNIST LeNet N=1000	Mean	98.8	96.6	98.7	98.8
	STD	3.1	5.2	3.2	3.1
	Min	75.0	57.1	75.0	75.0
	Max	100	100	100	100
CIFAR10 Conv8 N=1000	Mean	85.4	63.6	82.0	85.3
	STD	11.2	15.6	11.9	11.3
	Min	33.3	0	0	33.3
	Max	100	100	100	100
FEMNIST LeNet N=3400	Mean	85.8	69.2	82.9	84.2
	STD	10.2	14.2	11.1	10.7
	Min	10.0	0	14.3	7.1
	Max	100	100	100	100

In FRL, the weight parameters are randomly initialized at the start and remain fixed throughout the training. An appropriate initialization is instrumental to the success of FRL, since the FRL clients are sending the local rankings of these edges; more important edges get higher ranks. They generate these rankings by feeding the subnetwork of top rank edges and calculating the gradient of the loss with respect to the scores, so distribution of these random weights has a high impact on the calculated loss. We use three different distribution for initializing the weight parameters as follows:

Glorot Normal [20] where we denote by $\mathcal{X}_N$. Previous work [46] used this initialization to demonstrate that sub-

networks of randomly weighted neural networks can achieve impressive performance.

Kaiming Normal [21] where we denote by $\mathcal{N}_k$ defined as $\mathcal{N}_K = \mathcal{N}\left(0, \sqrt{2/n_{\ell-1}}\right)$ where $\mathcal{N}$ shows normal distribution. n_ℓ shows the number of parameters in the ℓth layer.

Singed Kaiming Constant [35] where all the weights are a constant σ but they are assigned $\{+, -\}$ randomly. This constant, σ, is the standard deviation of Kaiming Constant. We show this initialization with U_K as we are sampling from $\{-\sigma, +\sigma\}$ where $\sigma = \left(\sqrt{2/n_{\ell-1}}\right)$.

Table 5 shows the results of running FRL for three datasets under the three aforementioned initialization algorithms. We compare FRL with FedAvg and report the mean, standard deviation, minimum, and maximum of the accuracies for the clients' accuracies in FRL and FedAvg at the end of training. As we can see under three different random initialization, using Signed Kaiming Constant (U_K) results in better performance. We note from Table 5 that FRL with Signed Kaiming Constant (U_K) initialization achieves performance very close to the performance of FedAVg.

Note that, since the FRL clients update scores in each round, unlike initialization of weights, initialization of scores does not have significant impact on the final global subnetwork search. Therefore, we do not explore different randomized initialization algorithms for scores and simply use Kaiming Uniform initialization for scores.

Ramanujan et al. [35] also considered these three initialization to find the best subnetwork in centralized machine learning setting. They also showed that using Singed Kaiming Constant gives the best supermasks. Our results align with their conclusions, hence we use Singed Kaiming Constant to initialize the weights and Kaiming Uniform to initialize the scores of the global supernetwork.

7.5.3 FRL with varying sizes of subnetworks

In FRL, each client uses Edge-popup (Algorithm 1) and their local data to find a local ranking by finding a subnetwork within a randomly initialized global network, which we call *supernetwork*. Edge-popup algorithm uses parameter k which represents the % of all the edges in a supernetwork which will remain in the final subnetwork. For instance, $k = 50\%$ denotes that each client finds a subnetwork within a supernetwork that has half the number of edges as in the supernetwork.

Figure 5 illustrates how the performance of FRL varies with the sizes of local subnetworks that the clients share with the server. In other words, when we vary the sparsity $k\%$ of edge popup algorithm during local subnetwork search $k \in [10, 20, 30, 40, 50, 60, 70, 80, 90]\%$. Interestingly we note that, FRL performs the worst when clients use all (k=100%) or none (k=0%) of the edges. This is because, it is difficult to find a subnetwork with small number of edges. While using all of the edge essentially results in using a random neural
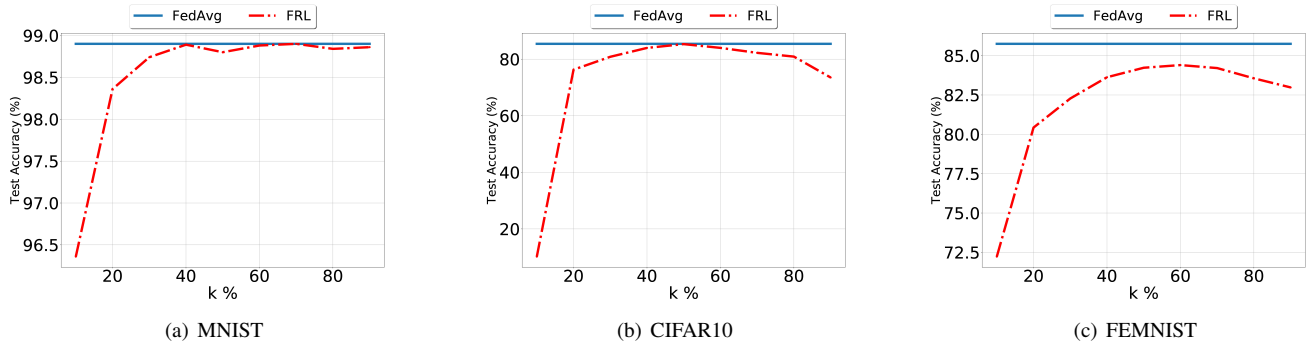
Figure 5: Comparing performance of FRL for different subnetwork sizes. k (x-axis) shows the % of weights that each client is including in its subnetwork, test accuracy (y-axis) shows the mean of accuracies for all the clients on their test data. The chosen clients in each round send all the ranks to the server. FRL with subnetworks of $\in [40\%, 70\%]$ result in better performances.

network. As we can see FRL with $k \in [40, 70]\%$, gives the best performances for all the three datasets. Hence, we set $k=50\%$ by default in our experiments.

7.5.4 FRL with larger networks

We already discussed the performance of the FRL for MNIST, CIFAR10, and FEMNIST datasets using moderately large neural networks with number of parameters ranging from 1.62M to 5.27M. In this section, we conduct experiments to demonstrate the effectiveness of FRL for very large networks: ResNet18 and ResNet34, with number of parameters 11.11M and 21.26M, respectively. Along with CIFAR10, we conduct experiments using a larger and significantly more challenging Tiny-ImageNet dataset. Table 7 shows the network architectures we use for these experiments. We have a batch normalization layer in these networks after each convolution layer. Following the setting of [14, 35, 43], we set the batch normalization to the non-affine mode, i.e., the scale and bias terms are set to $\gamma = 1$ and $\beta = 0$. We use the hyperparameters described in Section B.1 for all the models.

Tiny-ImageNet Table 6 shows the performance of FRL and FedAvg on Tiny-ImageNet for different network sizes, where ResNet18 and ResNet34 have 11.26 and 21.36 millions parameters respectively. From this table, we can see that FRL can achieve similar accuracy as FedAvg; for example, by using ResNet18, FRL achieves 31.0% test accuracy while FedAvg achieves 30.8% test accuracy.

CIFAR10. In Table 6, we show the final test accuracy of different models, Conv8 with 5.27M parameters, ResNet18 with 11.11M parameters, and ResNet34 with 21.26M parameters. We can see that FRL can achieve similar test accuracies as FedAvg for different model sizes. For example, For ResNet18, FRL achieves 89.3% test accuracy while FedAvg achieves 89.9% test accuracy.

8 Conclusions

We designed a novel collaborative learning algorithm, called Federated Rank Learning (FRL), to address the issues of robustness to poisoning and communication efficiency in existing FL algorithms. We argue that a core reason for the susceptibility of existing FL algorithms to poisoning is the large continuous space of values in their model updates. Hence, in FRL, we use ranks of edges of a randomly initialized neural network contributed by collaborating clients to find a global ranking and then use a subnetwork based only on the top edges. Use of rankings in a fixed range restricts the space available to poisoning adversaries to craft malicious updates, and also allows FRL to reduce the communication cost. We show, both theoretically and empirically, that ranking based collaborative learning can effectively mitigate the robustness issue as well as reduce the communication costs involved.

Table 6: FRL with larger networks for CIFAR10 and Tiny-ImageNet distributed over 1000 FL clients.

Dataset	Network	# of Params	FRL Acc (%)	FedAvg Acc (%)
CIFAR10 $N = 1000$	Conv8	5.27M	85.3	85.4
	ResNet18	11.11M	89.3	89.9
	ResNet34	21.26M	90.2	91.4
Tiny-ImageNet $N = 1000$	ResNet18	11.26M	31.0	30.8
	ResNet34	21.36M	30.9	30.8

References

[1] Tiny imagenet challenge [online]. https://tinyimagenet.herokuapp.com.

[2] Alham Fikri Aji and Kenneth Heafield. Sparse communication for distributed gradient descent. In *EMNLP*, 2017.

[3] Dan Alistarh, Torsten Hoefler, Mikael Johansson, Nikola Konstantinov, Sarit Khirirat, and Cédric Renggli. The convergence of sparsified gradient methods. In *NeurIPS*, 2018.

[4] Eugene Bagdasaryan, Andreas Veit, Yiqing Hua, Deborah Estrin, and Vitaly Shmatikov. How to backdoor federated learning. In *AISTATS*, 2020.

[5] Moran Baruch, Baruch Gilad, and Yoav Goldberg. A little is enough: Circumventing defenses for distributed learning. In *NeurIPS*, 2019.

[6] Yoshua Bengio, Nicholas Léonard, and Aaron Courville. Estimating or propagating gradients through stochastic neurons for conditional computation. *arXiv preprint arXiv:1308.3432*, 2013.

[7] Jeremy Bernstein, Jiawei Zhao, Kamyar Azizzadenesheli, and Anima Anandkumar. signsgd with majority vote is communication efficient and fault tolerant. In *ICLR*, 2019.

[8] Arjun Nitin Bhagoji, Supriyo Chakraborty, Prateek Mittal, and Seraphin Calo. Analyzing federated learning through an adversarial lens. In *ICML*, 2019.

[9] Peva Blanchard, Rachid Guerraoui, Julien Stainer, et al. Machine learning with adversaries: Byzantine tolerant gradient descent. In *NeurIPS*, pages 119–129, 2017.

[10] Keith Bonawitz, Hubert Eichner, Wolfgang Grieskamp, Dzmitry Huba, Alex Ingerman, Vladimir Ivanov, Chloé Kiddon, Jakub Konecnỳ, Stefano Mazzocchi, H Brendan McMahan, et al. Towards federated learning at scale: System design. In *MLSys*, 2019.

[11] Sebastian Caldas, Peter Wu, Tian Li, Jakub Konečný, H. Brendan McMahan, Virginia Smith, and Ameet Talwalkar. LEAF: A benchmark for federated settings. *CoRR*, abs/1812.01097, 2018.

[12] Francesco Paolo Cantelli. Sui confini della probabilita. In *Atti del Congresso Internazionale dei Matematici: Bologna del 3 al 10 de settembre di 1928*, pages 47–60, 1929.

[13] Hongyan Chang, Virat Shejwalkar, Reza Shokri, and Amir Houmansadr. Cronus: Robust and heterogeneous collaborative learning with black-box knowledge transfer, 2019.

[14] Daiki Chijiwa, Shin'ya Yamaguchi, Yasutoshi Ida, Kenji Umakoshi, and Tomohiro Inoue. Pruning randomly initialized neural networks with iterative randomization. *Advances in Neural Information Processing Systems*, 34:4503–4513, 2021.

[15] Gregory Cohen, Saeed Afshar, Jonathan Tapson, and André van Schaik. EMNIST: extending MNIST to handwritten letters. In *2017 International Joint Conference on Neural Networks, IJCNN*, 2017.

[16] Yann N Dauphin and Yoshua Bengio. Big neural networks waste capacity. *arXiv preprint arXiv:1301.3583*, 2013.

[17] Misha Denil, Babak Shakibi, Laurent Dinh, Marc'Aurelio Ranzato, and Nando de Freitas. Predicting parameters in deep learning. In *Proceedings of the 26th International Conference on Neural Information Processing Systems-Volume 2*, pages 2148–2156, 2013.

[18] Minghong Fang, Xiaoyu Cao, Jinyuan Jia, and Neil Zhenqiang Gong. Local model poisoning attacks to byzantine-robust federated learning. In *USENIX Security*, 2020.

[19] Jonathan Frankle and Michael Carbin. The lottery ticket hypothesis: Finding sparse, trainable neural networks. *ICLR*, 2019.

[20] Xavier Glorot and Yoshua Bengio. Understanding the difficulty of training deep feedforward neural networks. In *AISTATS*, 2010.

[21] Kaiming He, Xiangyu Zhang, Shaoqing Ren, and Jian Sun. Delving deep into rectifiers: Surpassing human-level performance on imagenet classification. In *Proceedings of the IEEE international conference on computer vision*, pages 1026–1034, 2015.

[22] Tzu-Ming Harry Hsu, Hang Qi, and Matthew Brown. Measuring the effects of non-identical data distribution for federated visual classification. *arXiv preprint arXiv:1909.06335*, 2019.

[23] Nikita Ivkin, Daniel Rothchild, Enayat Ullah, Vladimir Braverman, Ion Stoica, and Raman Arora. Communication-efficient distributed sgd with sketching. In *NeurIPS*, 2019.

[24] Peter Kairouz, H Brendan McMahan, Brendan Avent, Aurélien Bellet, Mehdi Bennis, Arjun Nitin Bhagoji, Keith Bonawitz, Zachary Charles, Graham Cormode, Rachel Cummings, et al. Advances and open problems in federated learning. *arXiv preprint arXiv:1912.04977*, 2019.

[25] Jakub Konečný, H Brendan McMahan, Felix X Yu, Peter Richtárik, Ananda Theertha Suresh, and Dave Bacon. Federated learning: Strategies for improving communication efficiency. *arXiv preprint arXiv:1610.05492*, 2016.

[26] Alex Krizhevsky and Geoffrey Hinton. Learning multiple layers of features from tiny images. 2009.

[27] Ang Li, Jingwei Sun, Binghui Wang, Lin Duan, Sicheng Li, Yiran Chen, and Hai Li. Lotteryfl: Personalized and communication-efficient federated learning with lottery ticket hypothesis on non-iid datasets. *CoRR*, 2020.

[28] Ang Li, Jingwei Sun, Xiao Zeng, Mi Zhang, Hai Li, and Yiran Chen. Fedmask: Joint computation and communication-efficient personalized federated learning via heterogeneous masking. In *Proceedings of the 19th ACM Conference on Embedded Networked Sensor Systems*, pages 42–55, 2021.

[29] Tian Li, Anit Kumar Sahu, Manzil Zaheer, Maziar Sanjabi, Ameet Talwalkar, and Virginia Smith. Federated optimization in heterogeneous networks. *arXiv preprint arXiv:1812.06127*, 2018.

[30] Heiko Ludwig, Nathalie Baracaldo, Gegi Thomas, and Yi Zhou. IBM federated learning: an enterprise framework white paper V0.1. *CoRR*, abs/2007.10987, 2020.

[31] H Brendan McMahan, Eider Moore, Daniel Ramage, Seth Hampson, and Blaise Aguera y Arcas. Communication-efficient learning of deep networks from decentralized data. *AISTATS*, 2017.

[32] El Mahdi El Mhamdi, Rachid Guerraoui, and Sébastien Rouault. The hidden vulnerability of distributed learning in byzantium. In *ICML*, 2018.

[33] Hamid Mozaffari, Virendra J Marathe, and Dave Dice. Fedperm: Private and robust federated learning by parameter permutation. *arXiv preprint arXiv:2208.07922*, 2022.

[34] Matthias Paulik, Matt Seigel, and Henry Mason. Federated evaluation and tuning for on-device personalization: System design & applications. *arXiv preprint arXiv:2102.08503*, 2021.

[35] Vivek Ramanujan, Mitchell Wortsman, Aniruddha Kembhavi, Ali Farhadi, and Mohammad Rastegari. What's hidden in a randomly weighted neural network? In *Proceedings of the IEEE/CVF Conference on Computer Vision and Pattern Recognition*, 2020.

[36] Vivek Ramanujan, Mitchell Wortsman, Aniruddha Kembhavi, Ali Farhadi, and Mohammad Rastegari. What's

hidden in a randomly weighted neural network? In *Proceedings of the IEEE/CVF Conference on Computer Vision and Pattern Recognition*, pages 11893–11902, 2020.

[37] Sashank J Reddi, Zachary Charles, Manzil Zaheer, Zachary Garrett, Keith Rush, Jakub Konečný, Sanjiv Kumar, and Hugh Brendan McMahan. Adaptive federated optimization. In *ICLR*, 2020.

[38] Virat Shejwalkar and Amir Houmansadr. Manipulating the byzantine: Optimizing model poisoning attacks and defenses for federated learning. In *NDSS*, 2021.

[39] Virat Shejwalkar, Amir Houmansadr, Peter Kairouz, and Daniel Ramage. Back to the drawing board: A critical evaluation of poisoning attacks on federated learning. In *Security and Privacy (SP)*. 2021.

[40] Sebastian U Stich, Jean-Baptiste Cordonnier, and Martin Jaggi. Sparsified sgd with memory. In *NeurIPS*, 2018.

[41] Ziteng Sun, Peter Kairouz, Ananda Theertha Suresh, and H Brendan McMahan. Can you really backdoor federated learning? In *NeurIPS FL Workshop*, 2019.

[42] Hongyi Wang, Kartik Sreenivasan, Shashank Rajput, Harit Vishwakarma, Saurabh Agarwal, Jy-yong Sohn, Kangwook Lee, and Dimitris Papailiopoulos. Attack of the tails: Yes, you really can backdoor federated learning. In *NeurIPS*, 2020.

[43] Mitchell Wortsman, Vivek Ramanujan, Rosanne Liu, Aniruddha Kembhavi, Mohammad Rastegari, Jason Yosinski, and Ali Farhadi. Supermasks in superposition. In *NeurIPS*, 2020.

[44] Chulin Xie, Keli Huang, Pin-Yu Chen, and Bo Li. Dba: Distributed backdoor attacks against federated learning. In *ICLR*, 2019.

[45] Dong Yin, Yudong Chen, Kannan Ramchandran, and Peter L. Bartlett. Byzantine-robust distributed learning: Towards optimal statistical rates. In *ICML*, 2018.

[46] Hattie Zhou, Janice Lan, Rosanne Liu, and Jason Yosinski. Deconstructing lottery tickets: Zeros, signs, and the supermask. In *NeurIPS*, 2019.

A   Theoretical analysis of FRL's robustness

In this section, we detail the proof of robustness of FRL. In other words, we prove an upper bound on the failure probability of robustness of FRL, i.e., the probability that a good edge will be removed from the final subnetwork when malicious clients mount the worst case attack. Following SignSGD [7], for this proof, we assume a simpler VOTE(.) function where

if more than half of the clients add an edge e_i to their subnetworks, then FRL server adds it to the final global subnetwork. We also assume that the malicious clients do not collude.

Assume that edge e_i is a good edge, i.e., having e_i in the final subnetwork improves the performance of the final subnetwork. Let Z be the random variable that represents the number of clients who vote for the edge e_i to be in the final subnetwork, i.e., the number of clients whose local subnetwork of size $k\%$ of the entire supernetwork (Algorithm 2 line 11) contains e_i. Therefore, $Z \in [0,n]$ where n is the number of clients being processed in a given FRL round.

Let G and B be the random variable that represent the number of benign and malicious clients that vote for edge e_i, respectively; the malicious clients inadvertently exclude the good edge e_i in their local subnetwork based on their benign training data.

There are total of αn malicious clients, where α is the fraction of malicious clients that B of them decides that e_i is a bad edge and should not be removed. Each of the malicious clients computes the subnetwork on its own benign training data, so B of them do not conclude that e_i is a good edge. Hence, $Z = G + B$. We can say that G and B have binomial distribution , i.e., $G \sim \text{binomial}([(1-\alpha)n, p]$ and $B \sim \text{binomial}([\alpha n, 1-p]$ where p is the probability that a benign client has this edge in their local subnetwork and α is the fraction of malicious clients. Note that the probability that our voting in simplified FRL fails is $P[\text{failure}] = P[Z <= \frac{n}{2}]$, i.e., when more than half of the clients vote against e_i, i.e., they do not include e_i in their local subnetworks. We can find the mean and variance of Z as follows:

$$E[Z] = (1-\alpha)np + \alpha n(1-p) \qquad (2)$$

$$Var[Z] = (1-\alpha)np(1-p) + \alpha np(1-p) = np(1-p) \quad (3)$$

[12] provides an inequality where for a random variable X with mean μ and variance σ^2 we have $P[\mu - X >= \lambda] <= \frac{1}{1+\frac{\lambda^2}{\sigma^2}}$. Using this inequality, we can write:

$$P[Z <= \frac{n}{2}] = P[E[Z] - Z >= E[Z] - n/2] <= \frac{1}{1 + \frac{(E[z]-n/2)^2}{var[Z]}}$$
$$(4)$$

because $1 + x^2 >= 2x$, we have:

$$P[Z <= \frac{n}{2}] <= 1/2\sqrt{\frac{Var[Z]}{(E[Z]-n/2)^2}} \qquad (5)$$
$$= 1/2\sqrt{\frac{np(1-p)}{(np - \alpha np + \alpha n - \alpha np - n/2)^2}}$$
$$= 1/2\sqrt{\frac{np(1-p)}{(n(p + \alpha(1-2p) - 1/2))^2}}$$

What this means is that the probability that the simplified VOTE(.) fails is upper bounded as in (5). We show the effect of the different values of α and p in Figure 3. We can see from Figure 3, if the benign clients can train better supermasks (better chance that a good edge ended in their subnetwork), the probability that the attackers succeed is lower (more robustness). VOTE(.) in FRL (Section 4.3) is more sophisticated and puts more constraints on the malicious clients, hence the about upper bound also applies to FRL.

B Additional details on experimental setup

In this section, we provide the details of experimental setup that are missing from Section 7.

B.1 Datasets and model architectures

We use four benchmark datasets widely used in prior works on federated learning robustness:

MNIST is a 10-class class-balanced classification task with 70,000 gray-scale images, each of size 28×28. We experiment with LeNet architecture given in Table 7. For local training in each FRL/FL round, each client uses 2 epochs. For training weights (experiments with FedAvg, SignSGD, TopK), we use SGD optimizer with learning rate of 0.01, momentum of 0.9, weight decay of 1e-4, and batch size 8. For training ranks (experiments with FRL), we use SGD with learning rate of 0.4, momentum 0.9, weight decay 1e-4, and batch size 8.

CIFAR10 [26] is a 10-class classification task with 60,000 RGB images (50,000 for training and 10,000 for testing), each of size 32×32. We experiment with a VGG-like architecture given in Table 7, which is identical to what [35] used. For local training in each FRL/FL round, each client uses 5 epochs. For training weights (experiments with FedAvg, SignSGD, TopK), we use SGD with learning rate of 0.1, momentum of 0.9, weight decay of 1e-4, and batch size of 8. For training ranks (experiments with FRL), we optimize SGD with learning rate of 0.4, momentum of 0.9, weight decay of 1e-4, and batch size of 8.

FEMNIST [11, 15] is a character recognition classification task with 3,400 clients, 62 classes (52 for upper and lower case letters and 10 for digits), and 671,585 gray-scale images. Each client has data of their own handwritten digits or letters. We use LeNet architecture given in Table 7. For local training in each FRL/FL round, each client uses 2 epochs. For training weights (experiments with FedAvg, SignSGD, TopK), we use SGD with learning rate of 0.15, momentum of 0.9, weight decay of 1e-4, and batch size of 10. For training ranks (experiments with FRL), we optimize SGD with learning rate of 0.2, momentum of 0.9, weight decay of 1e-4, and batch size of 10.

Tiny-ImageNet [1] contains 100K, 10k, 10k training, validation and test images respectively for 200 classes downsized to 64×64 colored images, so each class has 500 training, and

Table 7: In our experiments, we use the following, state-of-the-art model architectures from [14, 35, 43].

Architecture	Layer Name	Number of parameters
LeNet [43] (MNIST and FEMNIST)	Conv(32)	288
	Conv(64)	18432
	FC(128)	1605632
	FC(10) or FC(62)	1280 or 7936
Conv8 [35] (CIFAR10)	Conv(64), Conv(64)	38592
	Conv(128), Conv(128)	221184
	Conv(256), Conv(256)	884736
	Conv(512), Conv(512)	3538944
	FC(256), FC(256), FC(10)	592384
ResNet18 [43] (CIFAR10 and Tint-ImageNet)	Conv(64), [Conv(64), Conv(64)] $\times$ 2	149184
	[Conv(128), Conv(128)] $\times$ 2	524288
	[Conv(256), Conv(256)] $\times$ 2	2097152
	[Conv(512), Conv(512)] $\times$ 2	8388608
	Avg-Pool	-
	FC(10) or FC(200)	5120 or 102400
ResNet34 [43] (CIFAR10 and Tint-ImageNet)	Conv(64), [Conv(64), Conv(64)] $\times$ 3	222912
	[Conv(128), Conv(128)] $\times$ 4	1114112
	[Conv(256), Conv(256)] $\times$ 6	6815744
	[Conv(512), Conv(512)] $\times$ 3	13107200
	Avg-Pool	-
	FC(10) or FC(200)	5120 or 102400

50 validation and 50 test images. We distribute the training data over 1000 clients in a non-iid fashion using Dirichlet distribution with parameter $\beta = 1$. We run FedAvg and FRL for 4000 global rounds, and in each round, the FL server selects 25 clients randomly. For local training weights (experiments with FedAvg), we use SGD optimizer with a learning rate of 0.01, momentum 0.9, weight decays of 1e-5, batch size 8, and local epochs 2. For training ranks (experiment with FRL), we use SGD with a learning rate of 0.8, momentum of 0.9, weight decay of 1-e5, batch size 8, and local epochs 1. We optimize the hyperparameters based on the validation data and report the final accuracy on the test data.

B.2 Model architectures

Table 7 shows the state-of-the-art model architectures and corresponding datasets that we use in our experiments. We also show the number of parameters in each of their layers.

C FRL against targeted poisoning

So far, we evaluated the robustness of FRL against untargeted attacks. In this section, we evaluate the robustness against targeted poisoning, and specifically against *backdoor poisoning attacks*. We consider state-of-the-art backdoor attacks of three types: *semantic* [4], *artificial* [44], and *edge-case* [42] backdoor attacks. In this section, we first briefly discuss the three backdoor attack types; next, we discuss our evaluation setup, and finally, we present the experiment results at the end.

C.1 Existing FL backdoor attacks

Backdoor attacks [39] aim to misclassify *any* input that contains a specific signal called *backdoor trigger*, while correctly

(a) Semantic backdoor (b) Artificial backdoor (c) Edge-Case backdoor

Figure 6: Backdoor examples for different categories of targeted poisoning attacks on CIFAR10.

classifying inputs not containing the trigger. Based on the type of triggers, there are three kinds of backdoor attacks:
Semantic backdoor attacks [4] aim to misclassify a specific set of inputs that naturally contain a backdoor trigger. Figure 6(a) shows inputs from CIFAR10 data with the background of black stripes on a yellow wall as the naturally present, *semantic* trigger.
Artificial backdoor attacks [4, 44] aim to misclassify any input containing a manually added trigger. Figure 6(b) shows inputs with F shaped white pixels as the *artificial* trigger.
Edge-Case backdoor attacks [42] aim to misclassify inputs that are from the tail of the training data distribution. Hence, adversary can compute their model updates using mislabeled edge-case data and manipulate the global model to learn the incorrect correlation between data and labels. Figure 6(c) shows edge-case inputs for CIFAR10 distribution which are Southwest airplane images from Internet.

C.2 Evaluation setup

C.2.1 Training hyperparameters
We compare the performances of the FRL and FedAvg against the above backdoor attacks. We evaluate the accuracy of the (poisoned) global model on the main (inputs without trigger) and backdoor (inputs with trigger) tasks. Following [4, 42], for all the experiments, we start from a pre-trained model with 80.0% test accuracy and train it for 1,000 more FL rounds when malicious clients are present. We use $N = 1000$ clients, distribute CIFAR10 as in Section 7, and randomly select $n = 25$ clients in each round. We report the final test accuracy and the average of backdoor test accuracies over the 1000 FL rounds when percentages of malicious clients is in {1, 2, 5, 10}. We assume that each malicious client has some benign data (per the distribution scheme from Section 7) and all the backdoored data. We use the same hyperparameters discussed in Section 7 for training CIFAR10 on Conv8 model.

C.2.2 Backdoor attack hyperparameters

Model Replacement in FL backdoor Attacks: FL backdoor poisoning attacks use a strategy called model replacement where the malicious client first finds a malicious update that contains the backdoor, then it scales the model parameters to cancel the contributions from the other honest clients. For

example, if there are m malicious clients selected in FL round t, each malicious client u calculates its backdoored update θ_u^t, and re-scaled it to $\lambda \theta_u^t$ where $\lambda = \frac{m}{n}$ where n is the number of selected clients in each FL round. Model replacement strategy requires that the global model is close to convergence, so the malicious clients can replace the global model with their backdoored model, which performs well on the main task. Following this strategy, the backdoor accuracy would be very high in FedAvg, even if one of the malicious clients is chosen in one round. However, in FRL, re-scaling is not possible as the clients are sending their local rankings where each ranking are a permutation of the indices of the edges in each layer, i.e., of $[0, n_\ell - 1] \forall \ell \in [L]$ where L is the number of layers and n_ℓ is the number of parameters in ℓth layer. To have a fair comparison with FedAvg, we did not use a model replacement strategy for FedAvg too.

Semantic backdoors: We choose images with vertically striped walls in the background (Figure 7 (a)) as the backdoors. Of these 12 images with this trigger in the CIFAR10 dataset, we use 9 of them for training the backdoors while keeping the other three for testing the backdoor accuracy. The malicious clients want the global model to predict these images as the bird (class label=2). We measure the backdoor accuracy on 1000 randomly rotated and cropped versions of the three backdoor images held out of the adversary's training.

Artificial backdoors: We add a particular pixel pattern to the top left corner of the first nine (not bird) images of the CIFAR10 dataset (Figure 7 (b)) and change their labels to bird (label=2). To evaluate these attacks, we pick 256 random (not bird) images from CIFAR10 and add this pattern to them with the label of class bird.

Edge-Case backdoors: We collect 980 images from public web by searching for Southwest airplanes (similar to what [42] did) and resize the images to 32×32 (Figure 7 (c)). We set their target labels as truck (class label=9). We use 784 of these images for training and keep 196 of them for the evaluation of the backdoor.

C.3 Evaluation results

Semantic backdoor attacks: Figure 7 (a) shows the performance of FedAvg and FRL on the main task and the backdoor task when different percentages of malicious clients want to put a semantic backdoor in the global model. This figure shows that FRL is more robust against semantic backdoor attacks for different percentages of malicious clients. For example, with 2% of malicious clients, training FedAvg results in 84.4% final test accuracy with 82.7% average backdoor accuracy, while training FRL results in 84.1% and 49.2% accuracy on the main task and backdoor task, respectively. The existence of a more significant number of malicious clients (e.g., 10%) results in higher backdoor accuracy for both FedAvg and FRL as the malicious clients have more influence on the global model to introduce their backdoor; with existence of 10% of malicious clients, training FedAvg and FRL

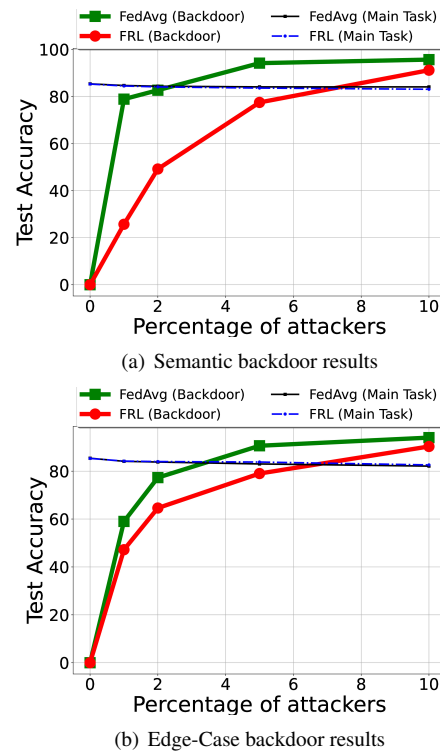achieves 95.7% and 91.2% average backdoor accuracy respectively.

(a) Semantic backdoor results

(b) Edge-Case backdoor results

Figure 7: FL backdoor poisoning attacks on CIFAR10 distributed over 1000 clients with Dirichlet ($\beta = 1.0$) for presence pf adversary in 1000 FL rounds.

Artificial backdoor attacks: These attacks are ineffective when the adversary cannot use model replacement strategy (i.e., cannot re-scale their parameters). In FRL, malicious clients cannot scale their updates, as they submit a local ranking (from a discrete space of updates). To be fair, we also did not use re-scaling in our experiments for FedAvg. We did not report the results for this attack, as the backdoor accuracy would be 0% for both FRL and FedAvg with no parameter re-scaling. It means that the global model always predict the right label (not the adversary target label "bird") for the test backdoor images.

Edge-Case backdoor attacks: Figure 7 (b) shows that FRL is more robust against Edge-case backdoor attacks for different percentages of malicious clients. For example, with 2% of malicious clients, training FedAvg results in 83.7% final test accuracy with 77.3% average backdoor accuracy, while training FRL results in 84.0% and 64.6% accuracy on the main task and backdoor task, respectively. Similar to semantic backdoors, a larger number of malicious clients (e.g., 10%) results in higher backdoor accuracy for both FedAvg and FRL; with 10% of malicious clients, training FedAvg and FRL achieves 94.0% and 90.3% average backdoor accuracy respectively.